International Journal of Pharmaceutics, 36 (1987) 17–28
Elsevier

IJP 01202

Locating the impurity in doped crystals using isotopic double labelling and a column "flow-through" dissolution cell: adipic acid doped with oleic acid

Joseph Go and David J.W. Grant

Faculty of Pharmacy, University of Toronto, Toronto, Ont. (Canada)

(Received 3 June 1986)
(Modified version received 3 October 1986)
(Accepted 20 October 1986)

Key words: Dissolution rate; Column dissolution; Solid solution; Impurity distribution; Double labeling; Crystal; Adipic acid; Oleic acid: Shape factor

Summary

A continuous-flow dissolution method employing a column is described for determining the relative distribution of an impurity or additive (guest molecules) present as a dopant in the crystals of a host substance. The host crystals were adipic acid, labelled with carbon-14, while the guest molecules were oleic acid, labelled with tritium. The dissolution of the doped crystals in acetonitrile, in which both adipic acid and oleic acid are soluble, was monitored by collecting fractions after short intervals of time (e.g. 30 s). The release of the guest and host were monitored concurrently using the different characteristic energies of their β-emissions. The release rates were expressed as functions of time and as functions of the percentage of the total mass of solid dissolved. The mole fraction of the guest molecules released, when plotted against the percentage of the total mass of solid dissolved, shows the distribution of the additive molecules relative to the host molecules. The method appears to be a useful addition to dissolution technology and may be adapted to monitor drug release from multiple drug formulations. The solubility of adipic acid in dry acetonitrile and the initial release rate of adipic acid into acetonitrile increased with increased doping with oleic acid suggesting an increased disruption of the crystal lattice. The release rate of the oleic acid dopant into acetonitrile rapidly decreased with time to a steady finite value indicating that, while some oleic acid was adsorbed onto the surface, a significant fraction was distributed throughout the crystals. The release rates of adipic acid from the crystals approximates to a biphasic linear function of the two-thirds power of the mass remaining, suggesting that dissolution is controlled by the available surface. The change in slope of the corresponding plots may be explained primarily by a change in the intrinsic solubility of the crystals during dissolution.

Introduction

The efficacy of a drug may be altered not only by the excipients that are used in compounding but also by the impurities and additives (guest molecules) present in solid solution in the particles of the pharmaceutical powders. Guest molecules in solid solution not only alter the shape of the host crystals (Fairbrother and Grant, 1978, 1979), but also their energy, density, surface and dissolution rate (Chow, A.H.L. et al., 1985; Chow, K.Y. et al., 1984, 1985, 1986). These effects will influence the processability and the bioavailability of the powder and hence the properties and behaviour of the final product (Hüttenrauch, 1978).

This study is mainly concerned with the loca-

Correspondence: D.J.W. Grant, Faculty of Pharmacy, University of Toronto, 19 Russell Street, Toronto, Ont., Canada M5S 1A1.

ation of the guest molecules (impurities or additives) in the host crystal: whether they are on the surface, or inside the crystal; and whether they are homogeneously dispersed or layered in definable patterns. To facilitate this, the host substance, adipic acid, was labelled with carbon-14 and the guest substance, oleic acid, with tritium. The dissolution of both components of the crystals was then measured, using the column "flow-through" dissolution cell (Langenbucher, 1969; Langenbucher and Rettig, 1977; Tingstad and Riegelman, 1970; Hanson, 1982), by the release of the radioactivity of each isotope into solution as a function of time. Precautions were taken to control the external variables so as to minimize, if not eliminate, their influence on the dissolution rates of the crystals, as presented in the next section. The selection of the column "flow-through" dissolution cell, although not an official testing apparatus, was primarily motivated by the following advantages. (a) The method is very reproducible and is often considered as one of the most useful alternatives to the present official methods (Langenbucher, 1969; Jones, 1980; Hanson, 1982). (b) Sink conditions are maintained during the dissolution process with certain precautions as to how the material is packed (Carstensen, 1983; Yonezawa and Carstensen, 1986). This is useful for substances of low solubility whose dissolved concentration would rapidly reach non-sink levels (> 10% of saturation) in the rotating basket or paddle methods, e.g. Apparatus 1 and 2 of U.S.P. XXI (1985). (c) The method enables dissolved fractions to be collected at very short time intervals for long periods at measurable concentrations. (d) The column method gives an improved hydrodynamic flow pattern, and thus avoids certain complications, such as those arising from agitation intensity (Collet et al., 1972), lack of constancy of stirring speed, position of the blades (Hanson, 1982), and viscosity changes in the medium (Riehl and Walz, 1975). (e) The actual instantaneous concentration of dissolved substance in this system is proportional to the instantaneous dissolution rate, i.e.

$$dm/dt = dV/dt \cdot c \quad (1)$$

where dm/dt = dissolution rate, dV/dt = the constant flow rate of the solvent and c = concentration of the dissolved substance. Thus, any change in dissolution rate may be monitored by the change in concentration at a constant flow rate. It should be emphasized that the flow rate must be controlled very accurately.

The use of double-labelling in these experiments addresses the problem of changes on solubilities, dissolution rates and variations between experiments. From *one* experiment the release of both adipic acid, A, and oleic acid, O, can be measured concurrently as a function of time, t, by applying Eqn. 1 to each substance, thus:

$$dm_A/dt = (dV/dt) \cdot c_A \quad (2)$$

$$dm_O/dt = (dV/dt) \cdot c_O \quad (3)$$

where c_A and c_O are the measured concentrations of A and O, respectively, in the effluent and where dm_A/dt and dm_O/dt are the derived released rates of adipic acid and oleic acid, respectively. The Results and Discussion section describes the methods of deriving: (a) the distribution of the additive molecules, oleic acid, relative to the host molecules, adipic acid, throughout the crystals; and (b) the overall composition of the crystals. All calculations were carried out on the Apple microcomputer (IIe and Macintosh), for which the softwares were specifically developed or purchased.

Materials and Methods

Reagents and chemicals

Adipic acid (A44) was purchased from Fisher Scientific, chloroform (8-9180) and acetonitrile (9017-3) from J.T. Baker Chemical Co., oleic acid (O-0750) from Sigma Chemical Co., and anhydrous ethanol (L9P15) from Commercial Alcohols. All were of the highest purity available commercially and were used without further purification. [1,6-^{14}C]Adipic acid (12040) was purchased from ICN Canada, Radio-isotope Division, and [9,10-^{3}H(N)]oleic acid (NET289) from NEN Canada. (N indicates the nominal position of the tritium label expected from the method of preparation.) Scintillation cocktail Ready-Solv HP/b

(158727) was purchased from Beckman Instruments, and water was distilled in an all-glass apparatus.

Preparation of crystals

Into a 500 ml round-bottomed flask were added 250 ml of distilled water, 25 g of adipic acid, 0.50 μCi of [^{14}C]adipic acid and 1.00 ml of an ethanolic solution containing various amounts of tritiated oleic acid. This mixture was maintained at 60°C in a water bath and stirred at 200 rpm for at least one hour with a teflon stirrer blade attached to a glass rod to ensure complete homogeneity. The water bath was of the refrigerated type (Haake D-19) with a thermostatically controlled heater/circulator (Haake E3-V) that kept the temperature constant to within 0.02°C. The mechanical stirrer was a Heidolph Digital model RZR-2000 equipped with a liquid crystal display (LCD); this enables the user to adjust the speed to within ± 1 rpm for various load requirements. With continued stirring, the thermostat was adjusted to 25°C and the refrigeration was switched on. Under these conditions the cooling was of zero-order with a rate constant of 0.194 K · min^{-1}. After 3 h the crystals formed were collected on a Buchner funnel (Whatman paper no. 4) under gentle suction, air-dried overnight and dried for 3 days over phosphorus pentoxide in vacuo. Yields of the dried crystals were 72–80% by weight. The crystals were then sieved: most were within the fractions 425–600 μm (28–35 mesh) and 600–710 μm (24–28 mesh).

Dissolution chamber

The dissolution rate of the crystals was determined using a "flow-through" dissolution cell, constructed from a cylindrical chromatographic column (Bio-Rad "Econocolumn", length 10 cm, diameter 1 cm) fitted with an adjustable flow adaptor (Fig. 1). The volume of the dissolution chamber can thus be varied as required by moving the adaptor up or down inside the column. The volume of the chamber should be as small as practically possible; too large a chamber causes diffusion of the dissolved solute into the incoming solvent.

Sieved (600–710 μm) and accurately weighed crystals (100 ± 4 mg) were placed inside the column and the flow adaptor was adjusted such that the chamber was 1 cm high (chamber volume = 0.785 ml). The dissolution medium was pumped up the column at 1 ml/min ($= dV/dt$) using a Gilson-302 HPLC pump via a Gilson-802B manometric module (a pulse damper), which minimized the pulse and ripple of the pump and the analytical errors and maximized the accuracy and constancy of the flow rate, dV/dt (Rock, 1979). The formation of air bubbles within the chamber was, of necessity, avoided. Bubbles will be formed if a non-wettable material is used inside the chamber, e.g. a teflon disc cannot be used with water. Chloroform, alcohols and acetonitrile give no wetting problem with teflon, nor do they dissolve teflon and teflon also does not contaminate these solvents. Ascending solvent flow is preferable to descending flow, since the former minimizes the formation of air bubbles and thus creates a more laminar flow of the solvent. Samples were taken at regular intervals (usually 0.5 ml every 30 s for 20

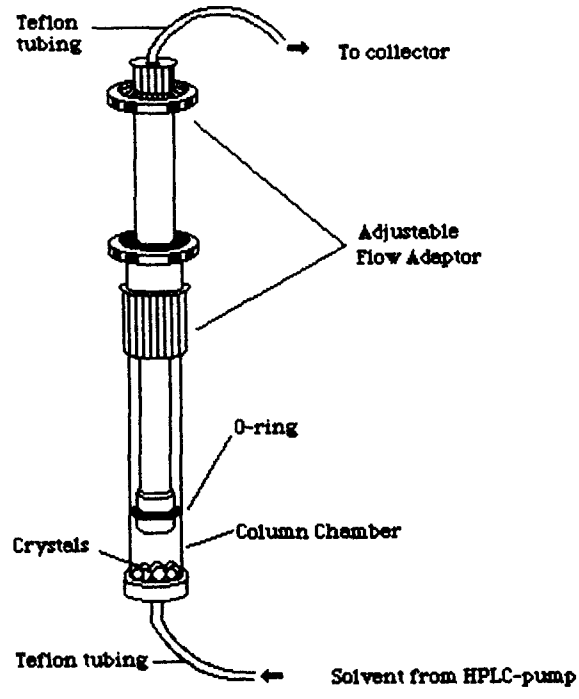

Fig. 1. Column type "flow-through" dissolution cell consisting of a cylindrical glass chromatographic column and a flow adaptor.

min). Each sample was mixed with 6.5 ml of scintillation cocktail (Beckman Ready-Solv HP/b). The radioactivity resulting from the β-decay was later counted as described below.

Radioactivity measurement

Radioactivity was measured using a Liquid Scintillation Counter (Beckman LS-7500) and counts were corrected using the "H-number" (Compton Edge) method with automatic quench compensation, AQC (Beckman, 1980). The amount of scintillation cocktail determines the degree of quenching inside the scintillation vial. The complications of dual-label corrections arise due to the presence of two β-emitting radionuclides with different energies. Dual-labelled samples must be counted in two channels, but the emission of β particles occurs over a range of energies for each radionuclide, causing some counts to spill over into the counting channel for the other radionuclide. The measured count rate in each channel results from the activity of both isotopes, although of course, one isotope predominates.

AQC is valuable in multiple-label counting because, in these instances, the accumulated counts in a particular channel arise from the joint contribution of several isotopes. In our case, where tritium and carbon-14 are counted, the counting channel which is set to monitor tritium will contain a significant portion of counts from carbon-14. Since we are using different solvent systems, quenching will vary from low to high levels in the samples. If quenching varies in a series of such samples, the carbon-14 contribution in the tritium channel will change and will then seriously affect the subsequent quench correction. By using AQC, however, the spillover of carbon-14 into the tritium channel is relatively constant.

Counting efficiency, E, is the ratio between the observed count rate in counts per minute (*cpm*) and the true activity in disintegrations per minute (*dpm*), thus:

$$E = cpm/dpm \tag{4}$$

Sample *cpm* values are converted to *dpm* values by using a quench curve, which is generated by counting known standards and plotting the efficiencies of the counting channels against a quench monitor, the *H*-number. Quench curves follow the third order of polynomial regression:

$$E = a + b \cdot H + c \cdot H^2 + d \cdot H^3 \tag{5}$$

where H = quench monitor, and a, b, c, and d are coefficients. When more than 5 standard samples are counted, the coefficients can be obtained by solving the system of normal equations derived from the least-squares principle. In this work, 8 standard samples of tritium and 10 of carbon-14

TABLE 1

Incorporation of [^{3}H]oleic acid, mole fraction, x_O[a], into [^{14}C]adipic acid crystals [b], and crystal designation

Crystal designation	Oleic acid		
	(mg/l) [c]	(μCi) [d]	($x_O \times 10^5$) [a]
CR1800	0.00	0.00	0.00
CR1803	3.33	18.64	3.56
CR1808	8.88	49.00	4.74
CR1817	17.77	98.70	7.75

[a] Calculated from Eqn. 20.
[b] Crystallized from aqueous solutions containing 100 g/l of adipic acid.
[c] Initial concentration of oleic acid in the crystallization solution.
[d] Activity of [^{3}H]oleic acid in the crystallization solution.

TABLE 2

Standards for tritium and carbon-14

Tritium standards			Carbon-14 standards		
H [a]	cpm_1 [b]	cpm_2 [c]	H [a]	cpm_1 [b]	cpm_2 [c]
250	13285.5	13884.2	300	1118.6	52152.1
222	28560.5	13176.3	260	3402.3	64387.7
160	73609.3	7789.1	217	7308.0	70894.6
134	98916.5	5749.1	168	12718.9	72987.4
92	144132.2	3230.6	139	18066.0	73381.8
66	177085.3	2028.8	99	18066.0	73287.5
40	210594.2	1548.4	75	19096.2	74830.1
0	260352.2	1815.0	42	21206.2	75114.5
			17	21106.2	76227.0
			3	20192.0	76264.0

[a] Quench monitor, the *H*-number; see Eqn. 5.
[b] Count rate in channel-1, in which β-emission from tritium predominates.
[c] Count rate in channel-2, in which β-emission from carbon-14 predominates.

were counted for this purpose (Table 2). Once the coefficients are known, any sample with known H-number can be interpolated or extrapolated to obtain its respective efficiency. When the dual-labelled sample is counted, in addition to the H-number, the count rates in channel-1 (cpm_1) and channel-2 (cpm_2) are obtained, thus:

$$cpm_1 = CH_1 + CC_1 \quad (6)$$

$$cpm_2 = CH_2 + CC_2 \quad (7)$$

where CH_1 = count of tritium in channel-1; CC_1 = count of carbon-14 in channel-1; CH_2 = count of tritium in channel-2; and CC_2 = count of carbon-14 in channel-2. Applying Eqn. 4 to Eqns. 6 and 7:

$$cpm_1 = DH \cdot EH_1 + DC \cdot EC_1 \quad (8)$$

$$cpm_2 = DH \cdot EH_2 + DC \cdot EC_2 \quad (9)$$

where DH = activity of tritium, DC = activity of carbon-14, EH_1 = efficiency of tritium in channel-1, EH_2 = efficiency of tritium in channel-2, EC_1 = efficiency of carbon-14 in channel-1 and EC_2 = efficiency of carbon-14 in channel-2. The activities of both tritium and carbon-14 (i.e. DH and DC, respectively) can thus be calculated by solving Eqns. 8 and 9 simultaneously.

Exchanges between tritium and hydrogen or between the isotopes of carbon in the compounds used in this work are very unlikely. The tritium is attached on the ethylenic group which would normally require a strong basic medium for an exchange to occur. The carbon-14, positioned at the carboxylic groups, is joined by a strong and stable covalent C–C bond that is unlikely to be broken by the methods used here.

Solubility

The equilibrium solubilities in acetonitrile of the doped and pure (control) crystals of adipic acid were determined as follows. One gram of crystals and 5.0 ml of acetonitrile were placed in a 7.0 ml screw-capped scintillation vial, vortexed for 1 min, sonicated for 2 min and allowed to equilibrate in dry air in an air-conditioned room at 22°C. Samples of 0.1 ml were taken at 3-day intervals with a positive-displacement pipette (Eppendorf no. 4780) fitted with a cotton-filled tip. This ensures that no solid was transferred into the scintillation vials. Each sample was mixed with 6.5 ml of scintillation cocktail and its radioactivity was measured as described above. After correction for quenching, the concentration of adipic acid in solution was calculated by comparison with a series of 5 known standards. The measured concentrations of adipic acid are shown in Table 3. The statistically significant increases in the solubility of the adipic acid crystals in acetonitrile with increased doping by oleic acid may reflect an increase in Gibbs free energy of the crystal lattice with its increasing disruption as a result of doping (Chow, K.Y. et al., 1984, 1985; Grant and York, 1986; Pikal and Grant, 1986). If this is the case, the initial dissolution rate of crystals of defined surface and size should also increase with increased doping with oleic acid (Chow, K.Y. et al., 1984, 1985, 1986; Grant and York, 1986), as observed in the present work to be discussed. The amounts of oleic acid released from the doped crystals in separate, control experiments are found to be insufficient, when mixed with the acetonitrile as solvent, to alter the measured solubility of adipic acid. This was demonstrated by equilibrating pure adipic acid crystals at 22°C in acetonitrile containing oleic acid at a range of concentrations from 0 to 100 μg/l. The measured solubilities of adipic acid were not statistically different from 9.71 ± 0.25 g/l stated in Table 3. Thus, the solubility differences shown in Table 3 are not a result

TABLE 3

Solubilities (g/l) of pure and doped crystals of adipic acid in acetonitrile at 22°C

Crystal designation	Number of measurements	Solubility ± S.D. ($P < 0.005$)
CR1800	12	9.71 ± 0.25
CR1803	5	11.07 ± 0.16
CR1808	5	13.00 ± 0.42
CR1817	5	18.57 ± 0.98

The crystals and solvent were equilibrated in scintillation vials kept in air (22°C) and samples were taken at 3-day intervals for 8 weeks.

TABLE 4

Values of slope, intercept, and other statistical parameters derived from Fig. 5 using Eqn. 18

Crystal	Phase [a]	Slope ± S.E. ($mg^{1/3} \cdot min^{-1}$)	Intercept ± S.E. ($mg \cdot min^{-1}$)	r^2	$s_{y.x}$	p_s
CR1800	1	0.071 ± 0.004	0.607 ± 0.062	0.921	0.060	0.0001
	2	0.142 ± 0.006	−0.248 ± 0.072	0.992	0.007	0.005
CR1803	1	0.035 ± 0.003	1.263 ± 0.051	0.952	0.010	0.0001
	2	0.084 ± 0.004	0.555 ± 0.053	0.953	0.041	0.0001
CR1808	1	0.056 ± 0.003	1.423 ± 0.055	0.919	0.054	0.0001
	2	0.189 ± 0.013	−0.032 ± 0.112	0.958	0.055	0.0001
CR1817	1	1.643 ± 0.063	−17.324 ± 0.937	0.990	0.475	0.0001
	2	0.270 ± 0.003	−1.111 ± 0.027	0.995	0.035	0.0001

[a] Phase 1 denotes the first linear period when the crystals were dissolving; phase 2 the subsequent linear period.

of the "salting in" of adipic acid by oleic acid at the concentrations employed.

Density

The true density of each batch of adipic acid crystals in Table 5 was determined by the flotation method using the following flotation liquids: 1-bromopropane, 1,1,2-trichloroethane and dichloromethane (Duncan-Hewitt and Grant, 1986). By this means the thermal expansivity of the crystals in Table 5 was also calculated. We note that increased doping with oleic acid does not change the density of these sets of adipic acid crystals, but appreciably decreases their thermal expansivity. This emphasizes the point made by Duncan-Hewitt and Grant (1986) that thermal expansivity may in certain cases provide a more sensitive indicator of crystal imperfection than density itself.

Results and Discussion

Choice of solvent

The adipic acid comprising the host crystals obtained from aqueous crystallization experiments was labelled with carbon-14, while the presence of tritiated oleic acid in the solution resulted in its uptake as guest molecules. The dissolution rate of

TABLE 5

Physical properties of pure and doped adipic acid crystals

Crystal	Phase	Slope [a] ($mg^{1/3} \cdot min^{-1}$)	Density [b] ($g \cdot cm^{-3}$)	Thermal expansivity [c] (K^{-1})	$k_s \cdot k$ [d] ($cm \cdot min^{-1}$)
CR1800	1	0.071	1.360	2.83×10^{-4}	0.90
	2	0.142	1.360	2.83×10^{-4}	1.80
CR1803	1	0.035	1.359	2.50×10^{-4}	0.39
	2	0.084	1.359	2.50×10^{-4}	0.93
CR1808	1	0.056	1.359	2.11×10^{-4}	0.53
	2	0.189	1.359	2.11×10^{-4}	1.78
CR1817	1	1.643	1.360	1.98×10^{-4}	10.86
	2	0.270	1.360	1.98×10^{-4}	1.78

[a] Taken from Table 4 and Fig. 5.

[b] Data determined using the flotation method for 22°C.

[c] Data determined at 3 temperatures using 3 flotation liquids.

[d] Apparent value, calculated from Eqn. 18, assuming that the solubility, c_A^s, is constant and given in Table 3.

the crystals as a function of time was determined using the continuous flow-through dissolution cell (Fig. 1) with acetonitrile as the solvent. In acetonitrile at 22°C the solubility of pure adipic acid is 10 g/l (Table 3), while that of oleic acid is found to be 74 g/l (1 : 12 v/v). The solubility data suggest that, when acetonitrile is used as the solvent, the adsorbed oleic acid is unlikely to present a significant barrier to the dissolution of the crystals. When, however, water is used as the solvent, the *adsorbed* oleic acid reduces the initial dissolution rate of the crystals, since the dissolution rate increases after the crystals have been washed with chloroform in which oleic acid is very soluble and adipic acid is sparingly soluble (Chow, K.Y. et al., 1985). When water is used as the flowing solvent in the present work, the mole fraction of oleic acid in the aqueous effluent is an irregular function of time; this arises from the very low solubility of oleic acid and its inherent hydrophobicity which causes it to be adsorbed by and to cling to the hydrophobic surfaces of the tubing walls (Fig. 1) forming small droplets that do not flow smoothly with the solvent. This pattern is not observed with acetonitrile or other solvents, e.g. alcohols, in which oleic acid is appreciably soluble. Therefore, when one of the components, e.g. oleic acid, is sparingly soluble in the solvent system, e.g. water, the mole fraction or molar ratio obtained from dissolution of crystals, e.g. adipic acid, may not represent the actual value within the crystal.

Dissolution rate

The dissolution of the doped and pure crystals of adipic acid in acetonitrile was monitored by collecting 0.5 ml samples of the effluent every 0.5 min for at least 20 min. Thus, Fig. 2 represents typical time plots of the release rates, dm_A/dt and dm_O/dt, which were derived using Eqns. 2 and 3 from the measured values of c_A and c_O, respectively, in the sample collected in each time interval, δt ($= 0.5$ min). Since the volume flow rate, dV/dt is constant, $dm_A/dt \propto c_A$ (Eqn. 2) and $dm_O/dt \propto c_O$ (Eqn. 3), the proportionality constant being $dV/dt = 1$ ml/min in each case. Fig. 2a and b show the actual plots of the dissolved concentrations, c_A and c_O, respectively,

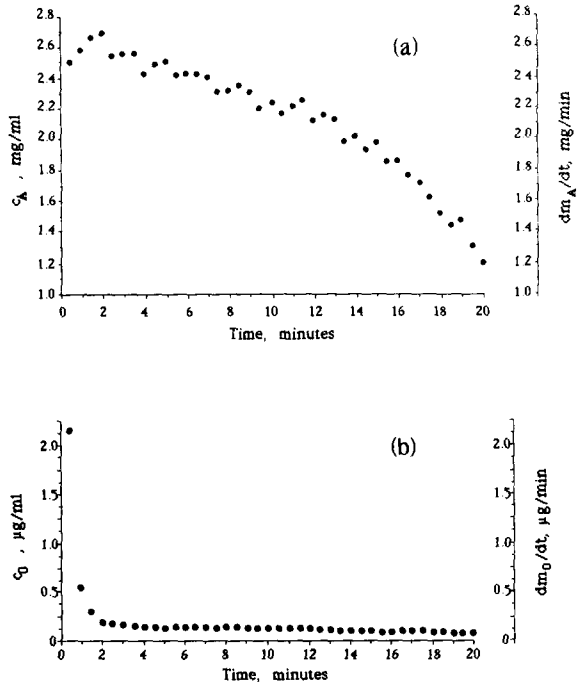

Fig. 2. Time plots of the effluent concentrations, c_A and c_O, and the release rates, dm_A/dt and dm_O/dt, of: (a) adipic acid, A; and (b) oleic acid, O, during the dissolution of the doped crystals CR1808 (Table 1) in acetonitrile at 22°C.

multiplied by this proportionality constant to give dm_A/dt and dm_O/dt, respectively.

The release rate of both adipic acid (Fig. 2a) and oleic acid (Fig. 2b) decreased with increasing time, probably because the surface area available for dissolution is decreasing as the crystals dissolve. The initial, relatively more rapid, decrease for dm_O/dt than for dm_A/dt suggests that oleic acid was concentrated at the surface during crystallization.

It might be thought that, if the column is full of crystals, there will be parts that are not in sink conditions (Carstensen, 1983; Yonezawa and Carstensen, 1986). The packing of the crystals inside the dissolution chamber is of little influence in the present work, since the amount of solid used is minimal, i.e. 100 mg, which barely covers the area of the disc.

The small mass increments of A released, δm_A, and of O released, δm_O, in each time interval, δt

(= 0.5 min), were calculated from the measured values of c_A and c_O, respectively, by means of Eqns. 2 and 3 in the following forms:

$$\delta m_A = (dV/dt) \cdot c_A \cdot \delta t \quad (10)$$

$$\delta m_O = (dV/dt) \cdot c_O \cdot \delta t \quad (11)$$

The total mass of A released, m_A, and of O released, m_O, up to time t may be obtained by adding together the individual increments of mass released in each time interval, δt, as follows:

$$m_A = \sum_0^t \delta m_A = \sum_0^t (dm_A/dt) \cdot \delta t \quad (12)$$

$$m_O = \sum_0^t \delta m_O = \sum_0^t (dm_O/dt) \cdot \delta t \quad (13)$$

The percentage, p, of the adipic acid crystals dissolved at each experimental value of t were derived from m_A, thus:

$$p = 100 \cdot m_A/m_{init} \quad (14)$$

where m_{init} is the initial mass of the crystals that were placed in the dissolution chamber. (Since m_O is only a tiny fraction of m_A, i.e. $x_O \ll x_A$, (Eqns. 19 and 20), m_A is a very close approximation to the actual mass of the crystal dissolved, $m_A + m_O$.) Fig. 3 shows plots of p against t corresponding to the data in Fig. 2 and derived from Table 4 using Eqns. 12 and 14. Fig. 3 represents cumulative dissolution profiles each of which may, of course, be derived directly from a typically batch-type dissolution experiment using Apparatus 1 or Apparatus 2 of the USP XXI (1985). Thus, the method described in the present report can provide the cumulative dissolution profiles which are commonly used in dissolution tests.

For each experimental value of t, the release rate dm_A/dt and dm_O/dt, are plotted against p in Fig. 4a and b. In view of the smooth dependence of p on t (Fig. 3) the general shape of the curves in Fig. 4 resemble those of Fig. 2. However, the percentage, p, of the crystals dissolved is a mass-related property of the dissolution experiment and therefore Fig. 4 is a mass-related version

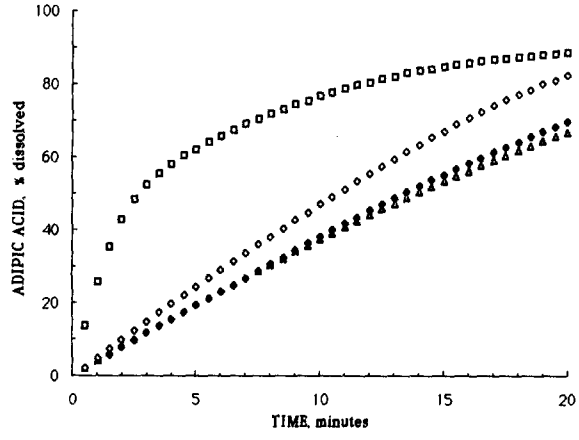

Fig. 3. Plots of the percentage, p, of adipic acid released against time during the dissolution of adipic acid crystals, (△) CR1800, (◆) CR1803, (◇) CR1808 and (□) CR1817 (Table 1) in acetonitrile at 22°C.

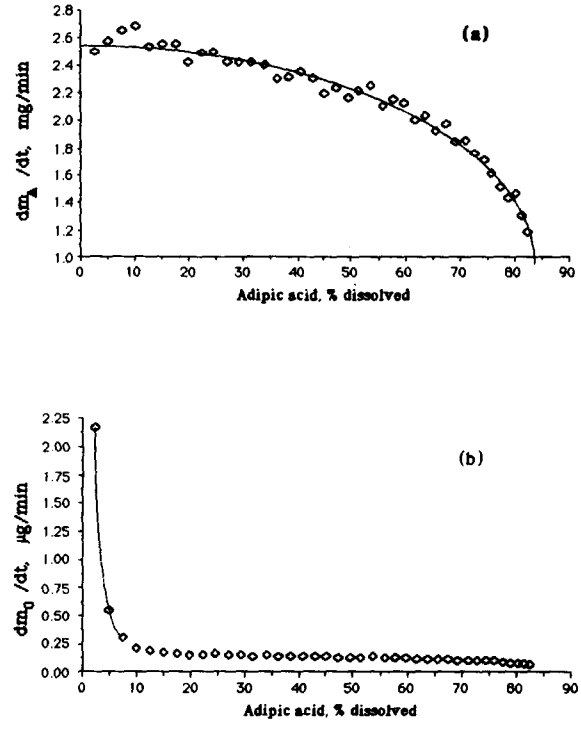

Fig. 4. Plots of the release rate of: (a) adipic acid; and (b) oleic acid against the percentage, p, of the crystals dissolved during the dissolution of the doped crystals CR1808 (Table 1 and Fig. 2) in acetonitrile at 22°C.

of Fig. 2. Since, however, the samples of the effluent from the dissolution column were collected at equal intervals of time, while the dissolution rate and mass of the crystals were decreasing, the points tend to become closer together with increasing p in Fig. 4a and b.

Under sink condition, the Noyes-Whitney (1897) equation may be written:

$$dm_A/dt = S \cdot k \cdot c_A^s \quad (15)$$

where S is the surface area, c_A^s is the solubility of A and k is the dissolution rate constant, which is a true constant only under fixed hydrodynamic conditions. For particles which maintain a similar shape

$$S = k_s \cdot V^{2/3} \quad (16)$$

where k_s is a shape factor (which is equal to $(36\pi)^{1/3} = 4.836$ for spheres and 6 for cubes) and V is the volume of the crystals remaining at time t. The mass remaining at time t, is given by $(m_{init} - m_A - m_O)$, where m_{init} is the initial mass of crystals present at $t = 0$. The mass remaining is related to V by the true density, ρ, of the crystals, thus:

$$V = (m_{init} - m_A - m_O)/\rho \quad (17)$$

Eliminating S and V from Eqns. 15–17 affords

$$dm_A/dt = k_s \cdot k \cdot \rho^{-2/3} \cdot c_A^s \cdot (m_{init} - m_A - m_O)^{2/3} \quad (18)$$

Arising from this equation, dm_A/dt is plotted against $(m_{init} - m_A - m_O)^{2/3}$ as shown in Fig. 5a–d. Any linear region in these plots indicates that $k_s \cdot k \cdot \rho^{-2/3} \cdot c_A^s$ is constant. Any change in slope suggest that one or more of the quantities k_s, k, $\rho^{-2/3}$, and c_A^s, is/are changing as the crystals dissolve. In general, each plot in Fig. 5a–d shows two approximately linear regions from which $k_s \cdot k \cdot \rho^{-2/3} \cdot c_A^s$ was calculated together with the statistics of linear regression; Table 4 shows these derived quantities. The density, ρ, and the solubility, c_A^s, of the adipic acid were determined in the present work (Table 3), whence the product of the constants k_s. k was calculated and is presented in Table 5. As a first approximation we assume that the density, ρ, and solubility, c_A^s, of a given batch of dissolving crystals is constant, in which case the change in slope in Fig. 5a–d probably reflects changes in k_s and/or k. Any change in shape during dissolution will probably reduce k_s, since the rate of dissolution is generally in the order corner > edge > face and results in more rounded crystals (Withey, 1971). This behaviour can explain the change in slope in Fig. 5d, but not that in Fig. 5a–c, which proceeds in the reverse direction. A change in shape or packing will also change the hydrodynamics of solvent flow and will therefore change the dissolution rate constant, k, but the effect will probably be relatively small. As mentioned earlier, the packing of the crystals (Yonezawa and Carstensen, 1986) inside the dissolution chamber is of little influence in the present work, since the amount of solid used is minimal, i.e. 100 mg, which barely covers the area of the disc.

The rather abrupt changes in slope in Fig. 5a–c are in a direction opposite to that predicted by a change in shape and that in Fig. 5d is much larger and more abrupt than expected from this cause. Hence another factor is probably responsible for the observed changes in the slope of the plots. This factor is unlikely to be the density of the solid, which generally changes very little on doping (Chow, K.Y. et al., 1985; Duncan-Hewitt and Grant, 1986). This leaves only the solubility, c_A^s, to account for the changes in slope in Fig. 5a–d. Table 3 shows that the solubility of the adipic acid crystals does indeed change on doping with oleic acid. The solubility reflects the free energy of the solid which increases with increasing lattice disruption. Thus, the changes in slope in Fig. 5a–d are better attributed to changes in intrinsic solubility, i.e. crystal defects, than to changes in crystal habit. It should be pointed out, however, that the "break point" in Fig. 5 (where the two straight lines intersect) is not related to any obvious features of the plot of the release of oleic acid vs time. The method of plotting Fig. 4 is too simplistic to investigate the factors influencing the dissolution process, which is the objective of presenting the measurements in the form of Fig. 5.

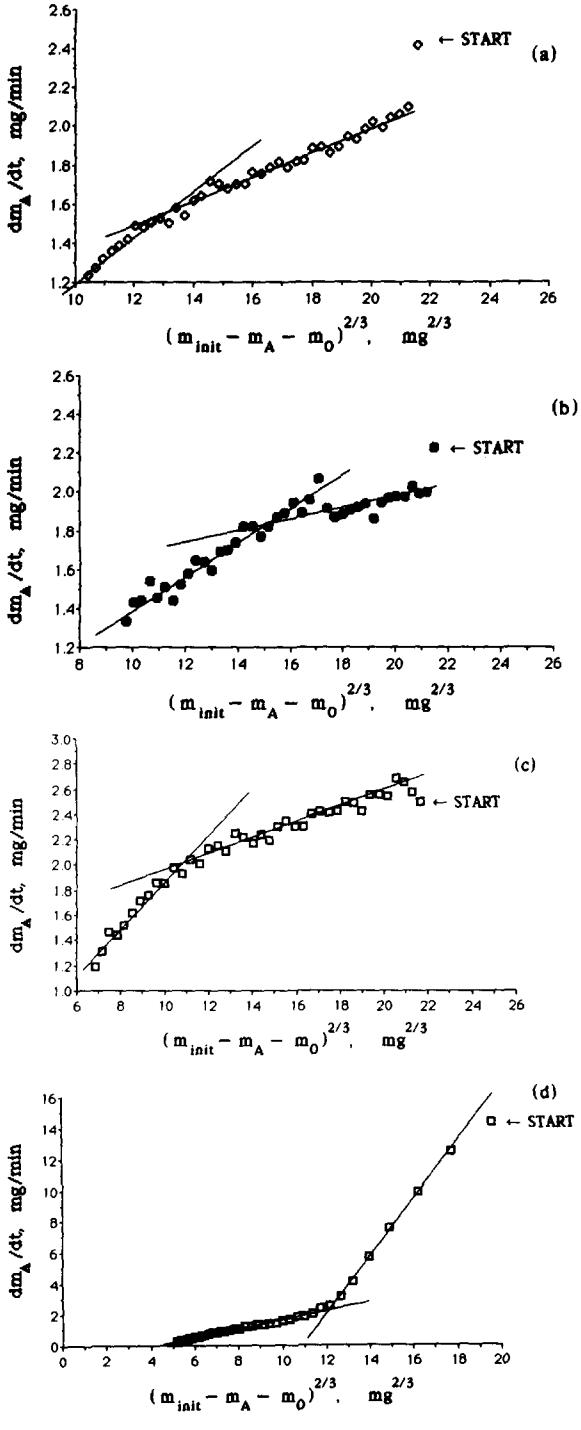

Fig. 5. Plots of the release rate against the mass remaining to the two-thirds power during the dissolution of the crystals: (a) CR1800; (b) CR1803; (c) CR1808; and (d) CR1817 in acetonitrile at 22°C.

The mole fraction of A, x_A, and of O, x_O, which were present in the increment of crystals that dissolved in each time interval, δt ($= 0.5$ min), were calculated from the values of c_A using Eqn. 10 and c_O using Eqn. 11, as follows:

$$x_A = \frac{\delta m_A/M_A}{\delta m_A/M_A + \delta m_O/M_O} = \frac{c_A/M_A}{c_A/M_A + c_O/M_O} \quad (19)$$

$$x_O = \frac{\delta m_O/M_O}{\delta m_A/M_A + \delta m_O/M_O} = \frac{c_O/M_O}{c_A/M_A + c_O/M_O} \quad (20)$$

where M_A is the molecular weight of adipic acid ($= 146.15$) and M_O is that of oleic acid ($= 282.47$). Since c_A and c_O were each assayed using the same sample in the same scintillation vial, the accuracy of x_A and x_O is limited only by the simultaneous determination of carbon-14 and tritium. The crystals in each dissolution experiment were of approximately the same granular shape and, as a result of sieving, of approximately the same size and were therefore presumably all dissolving at the same rate. If these conditions apply, then the plot of x_O against p in Fig. 6 represents the distribution of the additive throughout the doped crystal, from the surface at $p = 0\%$ to the centre of the crystal at $p = 100\%$. A straight horizontal line would represent an even distribution of the guest throughout the host crystal, whereas any peak represents preferential concentration at the corresponding value of p. Thus, in Fig. 6 the initial high values of x_O at small values of p indicate that the oleic acid is concentrated preferentially at the surface of the crystals of adipic acid. Later in the dissolution process, the approximately constant values of x_O at $p > 10\%$ for CR1803, at $p > 15\%$ for CR1808 and at $p > 45\%$ for CR1817 represent an even distribution of oleic acid throughout. On the other hand, the average composition of the crystals is given by the aggregate values of x_A and x_O when all the crystals have dissolved, which are represented by x_A^∞ and x_O^∞, respectively. Fig. 6 compares each value of x_O^∞ (right hand column in Table 1) with the corre-

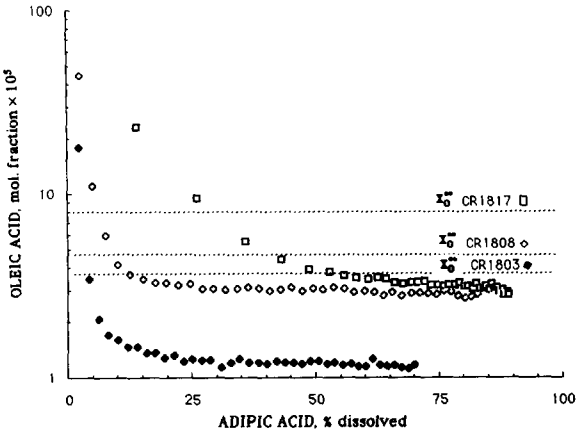

Fig. 6. Plots of the mole fraction, x_O, of oleic acid (log scale) released in 0.5 min against the percentage, p, of adipic acid during the dissolution of the doped crystals (◆) CR1803, (◇) CR1808 and (□) CR1817 in acetonitrile at 22°C.

sponding plateau value of x_O for each set of doped crystals. The fact that x_O^∞ is higher than the plateau value in each case suggests that the oleic acid, which is preferentially adsorbed on the surface, makes a significant contribution to x_O^∞.

The powder X-ray diffraction pattern of adipic acid crystals is not detectably changed after doping with oleic acid (Chow, K.Y. et al., 1985). This technique is not sensitive enough to determine: (a) whether or not the surface of the crystals is amorphous or constitutes a solid solution; and (b) the amount of doping required to maximize the effect on solubility. Suitable methods for answering these questions are at present under scrutiny.

Conclusions

(1) By labelling the impurity or additive (the guest substance) with one isotope and the major substance (the host) with another isotope, the release rate of both substances during the dissolution of the crystals can be monitored concurrently.

(2) When a continuous flow dissolution technique is used with a solvent in which both guest and host are appreciably soluble (i.e. acetonitrile, here), the distribution of the guest substance throughout the crystal mass can be determined.

(3) The above techniques can also be used to construct the usual dissolution–time profile of the solid as determined by the common batch methods (using a beaker and a stirrer or a rotating basket).

(4) When ^{14}C-labelled adipic acid crystals are grown in the presence of tritiated oleic acid, and when these crystals are dissolved in acetonitrile as above, the oleic acid is found to be distributed throughout the crystals, but an appreciable quantity is found to be adsorbed onto the surface of the crystals.

(5) The solubility of the adipic acid crystals in dry acetonitrile increases progressively with increased doping with oleic acid, suggesting an increase of free energy of the solid state with respect to the solution, presumably as a result of increasing disruption of the crystal lattice.

(6) The dissolution rate of the adipic acid from crystals approximates to a biphasic linear function of the two-thirds power of the mass remaining, suggesting that dissolution is controlled by the available surface of the solid. The changes in slope in the corresponding plots are better attributed to changes in the intrinsic solubility of the crystals during dissolution than to changes in shape of the crystals.

Acknowledgements

We thank Mrs. Wendy Duncan-Hewitt for carrying out the measurements of density and thermal expansivity and the Medical Council of Canada for an operating grant (MT-7835).

References

Beckman Instruments Inc., Applications of quench monitoring by Compton edge: the "H-Number". *Beckman Instruments Technical Reference* no. 1096-NUC-77-2T, 1980.

Carstensen, J.T., A model for dissolution of monodisperse powders from columns. *Labo-Pharma, Probl. Tech.*, 31 (1983) 10–12.

Chow, A.H.-L., Chow, P.K.K., Wang Zhongshan and Grant, D.J.W., Modification of acetaminophen crystals: influence of growth in aqueous solutions containing *p*-acetoxyacetanilide on crystal properties. *Int. J. Pharm.*, 24 (1985) 239–258.

Chow, K.Y., Go, J., Mehdizadeh, M. and Grant, D.J.W.,

Modification of adipic acid crystals: influence of growth in the presence of fatty acid additives on crystal properties. *Int. J. Pharm.*, 20 (1984) 3–24.

Chow, K.Y., Go, J., Wang Zhongshan, Mehdizadeh, M. and Grant D.J.W., Modification of adipic acid crystals: II. Influence of growth in the presence of oleic acid on crystal properties. *Int. J. Pharm.*, 25 (1985) 41–55.

Chow, K.Y., Go, J. and Grant D.J.W., Influence of fatty acid additives on the dissolution behavior of adipic acid crystals. *Drug Dev. Ind. Pharm.*, 12 (1986) 247–264.

Collet, J.H., Rees, J.A. and Dickinson, N.A., Some parameters describing the dissolution rate of salicylic acid at controlled pH. *J. Pharm. Pharmacol.*, 24 (1972) 724–728.

Duncan-Hewitt, W.C. and Grant, D.J.W., True density and thermal expansivity of pharmaceutical solids: comparison of methods and assessment of crystallinity. *Int. J. Pharm.*, 28 (1986) 75–84.

Fairbrother, J.E. and Grant D.J.W., The crystal habit modification of a tablet lubricant, adipic acid. *J. Pharm. Pharmacol.*, 30 Suppl. (1978) 19P.

Fairbrother, J.E. and Grant D.J.W., Crystal engineering studies with an excipient material (adipic acid). *J. Pharm. Pharmacol.*, 31 Suppl. (1979) 27P.

Grant, D.J.W. and York, P., A disruption index for quantifying the solid state disorder induced by additives or impurities. II. Evaluation from heat of solution. *Int. J. Pharm.*, 28 (1986) 103–112.

Hanson, W.A., *Handbook of Dissolution Testing*. Pharmaceutical Technology Publications. Springfield, OR, 1982, pp. 45–56.

Hüttenrauch, R., Molekulargalenik als Grundlage moderner Arzneiformung, *Acta Pharm. Technol.*, APV Informationsdienst Suppl. 6 (1978) 55–127.

Jones, T.M., The physico-technical properties of starting materials used in tablet formulation. *Int. J. Pharm. Technol. Prod. Mfr.*, 2 (1980) 17–24.

Jost, W., *Diffusion — Solids, Liquids and Gases*, Academic Press, New York, 1960, p. 78.

Langenbucher, F., In vitro assessment of dissolution kinetics: Description and evaluation of a column type method. *J. Pharm. Sci.*, 58 (1969) 1265–1272.

Langenbucher, F. and Rettig, H., Dissolution rate testing with the column method: methodology and results. *Drug Dev. Ind. Pharm.* 3 (1977) 241–263.

Pikal, M.J. and Grant, D.J.W., A theoretical treatment of changes in energy and entropy of solids caused by additives or impurities in solid solution. (1986) submitted.

Riehl, J. and Walz, H., Einfluss der Viskosität des Lösungsmittels auf die Lösungsgeschwindigkeit des Feststoffes. *Arch. Pharm.*, 309 (1975) 241–250.

Rock, J., Effect of pump ripple on quantitation and gradient performance. *Chromatogr. Rev.*, 5 (1979) 8–9.

Tingstad, J. and Riegelman, S., Dissolution rate studies I: Design and evaluation of a continuous flow apparatus. *J. Pharm. Sci.*, 59 (1970) 692–696.

U.S.P. XXI, *The United States Pharmacopeia*, 21st Revision, US Pharmacopeial Convention, Inc., Rockville, MD, 1985, pp. 1243–1244.

Withey, R.J., The kinetics of dissolution for a non-disintegrating standard substrate. *J. Pharm. Pharmacol.*, 23 (1971) 573–582.

Yonezawa, Y. and Carstensen, J.T., Dissolution profiles in column dissolution. *J. Pharm. Sci.*, 75 (1986) 764–768.